

Evidence for hydrogen-bond enhanced structural anomeric effects from the protonation of two aminals, 5-methyl-1,5,9-triazabicyclo[7.3.1]tridecane and 1,4,8,11-tetraazatricyclo[9.3.1.1^{4,8}]hexadecane



Roger W. Alder,^{*a} Tania M. G. Carniero,^a Rodney W. Mowlam,^a A. Guy Orpen,^a Peter A. Petillo,^c David J. Vachon,^b Gary R. Weisman^{*b} and Jonathan M. White^{a†}

^a School of Chemistry, University of Bristol, Bristol, UK BS8 1TS.

E-mail: rog.alder@bristol.ac.uk

^b Department of Chemistry, University of New Hampshire, Durham, NH 03824, USA.

E-mail: gary.weisman@unh.edu

^c Department of Chemistry, University of Illinois at Urbana-Champaign, 600 South Mathews Avenue, Urbana, Illinois 61801, USA

Received (in Cambridge) 13th October 1998, Accepted 22nd December 1998

The structure of the monoprotanated ion, **2**, of 5-methyl-1,5,9-triazabicyclo[7.3.1]tridecane, **1**, as a picrate shows an NMeH⁺ group engaged in a transannular hydrogen bond with one of the aminal nitrogen atoms and this, in turn, induces a small but measurable structural anomeric effect in the aminal functional group. Diprotonation of **1** in CF₃CO₂H yields an equilibrium mixture of two isomeric bicyclic dicationic species which are interconverted *via* a monocyclic ion containing a H₂C=N⁺ group and further protonation by CF₃SO₃H traps the iminium ion as a monocyclic trication. The structure of the monoprotanated ion, **4**, of 1,4,8,11-tetraazatricyclo[9.3.1.1^{4,8}]hexadecane, **3**, as a perchlorate shows the cation with effective C₂ symmetry, a nearly linear, and almost symmetrical, transannular hydrogen bond, and a more pronounced structural anomeric effect in both hexahydropyrimidine units. Diprotonation of **3** gives a dication, **5**, and the structure of the bis(trifluoroacetate) shows measurable shortening of the aminal C–NR₂ bond in spite of the fact that the lone pair and the C–N⁺ bond are close to *gauche*. The structural effects in **2**, **4**, and **5** are well-reproduced by Becke–Perdew density functional theory calculations, and a natural bond orbital analysis of the parent system H₃N–H⁺⋯NH₂CH₂NH₂, based on SCF and MP2 *ab initio* calculations is described.

Introduction

The anomeric effect^{1–7} is now generally accepted to be due, at least in part, to stabilising two-electron *n*→σ* interactions (sacrificial hyperconjugation),⁸ and these have been shown to give rise to structural anomeric effects which involve significant bond shortening/bond lengthening, as shown in Fig. 1(a), in a variety of RO–C–X structures where X is a good leaving group and the C–X bond is antiperiplanar to a lone pair on oxygen.^{9,10} The magnitude of these effects is expected to depend on the electronegativity of X. The first, reversible, step in the hydrolysis of acetals and related species is protonation and the cation formed should show a substantial structural anomeric effect, but RO–C–O(R)H⁺ ions are generally too unstable for structural studies. Simple analogy suggests that the same effects should apply to nitrogen-based species, with very small, or negligible effects for neutral aminals [Fig. 1(b)] where charge separation is involved, but substantial effects for R₂NCHRNR₃⁺ ions [Fig. 1(c)], provided that the lp–N–C–N⁺ torsion angle is close to 180° (antiperiplanar) or 0° (eclipsed). However, the situation for the nitrogen analogues has been confusing, since it was asserted that in RO–C–NR₃⁺ structures the conformational effects were reversed, so that the NR₃⁺ group showed an enhanced preference for the equatorial position in six-membered rings (the so-called reverse anomeric effect).^{1,11} Recent work, however, seems to have discredited this effect.^{12,13} In fact, evidence for a structural anomeric effect in R₂NCHRNR₃⁺ ions can be garnered from the Cambridge Crystallographic Database and will be discussed later. These

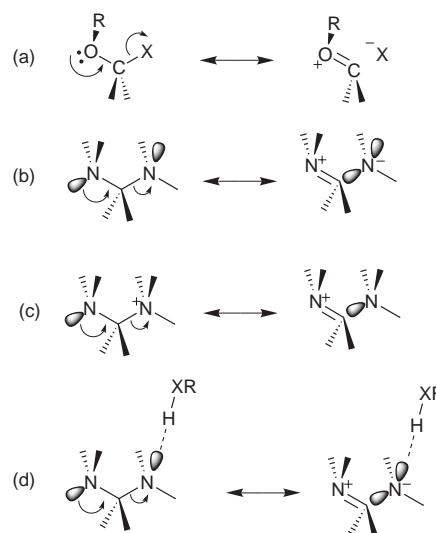
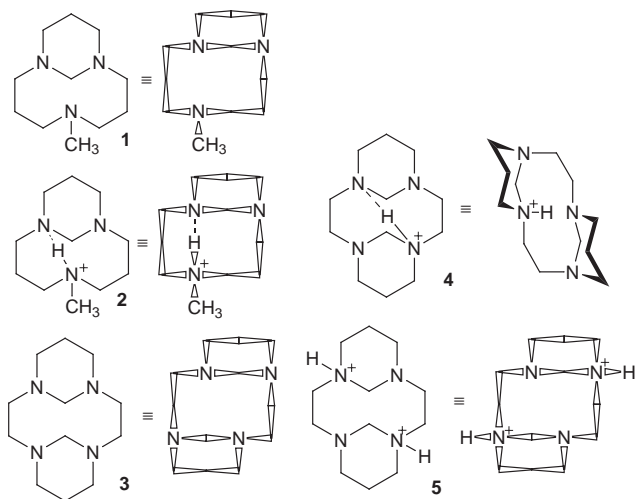


Fig. 1 Structural anomeric effects.

nitrogen-containing systems possess a major advantage, as far as interpretation is concerned, over the corresponding oxygen species in that, with only one lone pair per heteroatom, the lp–N–C–X torsion angles are easily and unequivocally determined.

In this paper, we show that for aminals (R₂NCH₂NR₂) even hydrogen bond formation to one of the nitrogen atoms is enough to induce measurable structural anomeric effects in the normal direction [see Fig. 1(d)], with the size of these effects being proportional to the strength of the hydrogen bond. We

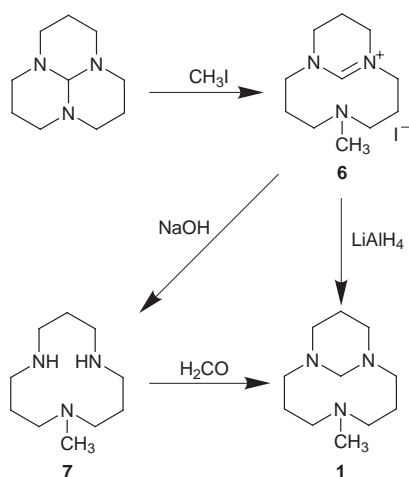
† Present address: School of Chemistry, University of Melbourne, Parkville VIC 3052, Australia.



report the structure of the picrate of monoprotonated ion, **2**, derived from 5-methyl-1,5,9-triazabicyclo[7.3.1]tridecane, **1**, possessing a relatively weak and unsymmetrical hydrogen bond, and the monoprotonated ion, **4**, of 1,4,8,11-tetraazatricyclo[9.3.1.1^{4,8}]hexadecane,^{14–16} **3**, as a perchlorate, which has a strong, potentially single-minimum (symmetrical) hydrogen bond. The structure of the diprotonated ion, **5**, of **3**, as a bis-(trifluoroacetate), possesses some intriguing features and is also reported, and the ions formed by further protonation of **1** are studied by NMR.

Experimental

The preparation of 1,4,8,11-tetraazatricyclo[9.3.1.1^{4,8}]hexadecane **3** was carried out by reaction of cyclam with formaldehyde as reported earlier.¹⁵ 5-Methyl-1,5,9-triazabicyclo[7.3.1]tridecane, **1** was prepared by two different routes, *via* intermediates **6** and **7** (Scheme 1), whose preparation has been briefly reported,¹⁷ but details are given below.



Scheme 1

5-Methyl-5,9-diaza-1-azoniabicyclo[7.3.1]tridec-1(13)-ene iodide, **6**

Iodomethane (213 mg) was added to a stirred solution of 1,5,9-triazatricyclo[7.3.1.0^{5,12}]tridecane¹⁸ (181 mg) in acetonitrile (5 cm³) and the reaction mixture stirred at room temperature for 1 h under nitrogen. The solvent and excess iodomethane were removed under reduced pressure to yield a white solid (quantitative yield), mp 234–238 °C (dec) (Found: C, 41.02; H, 7.13; N, 13.04%. C₁₁H₂₂N₃I requires C, 40.88; H, 6.86; N, 13.00%); δ_{H} (400 MHz; CDCl₃): 9.35 (s, 1H), 4.38 (ddd, 2H, $J = 12.5, 12.5, 2.4$ Hz), 3.45–3.25 (m, 8H), 2.64–2.58 (m,

2H), 2.37–2.18 (m, 5H), 2.09–2.00 (m, 2H), 1.46–1.41 (m, 2H); δ_{C} (67.8 MHz; CDCl₃): 158.4 (1C), 58.5 (2C), 54.3 (2C), 42.7 (2C), 41.8 (1C), 22.8 (2C), 19.9 (1C); IR (Nujol): 1670, 1422, 1328, 1220, 1115, 1040, 857, 667 cm⁻¹.

1-Methyl-1,5,9-triazacyclododecane, **7**

Amidinium salt **6** (0.969 g) was dissolved in distilled water (5 cm³), 10% sodium hydroxide (5 cm³) was added and the solution refluxed for 20 h. The reaction solution was cooled, extracted with chloroform (3 × 20 cm³) and dried over sodium sulfate. The solvent was removed under reduced pressure and the crude product (a yellow oil) Kugelrohr distilled (90 °C, 0.25 Torr) to yield a hygroscopic low melting crystalline solid (350 mg, 63.1%) [Found (EI): M⁺, 185.1887. C₁₀H₂₃N₃ requires 185.1892]; δ_{H} (60 MHz; CDCl₃): 3.50 (bs, 2H, NH), 2.90–2.25 (m, 12H), 2.10 (s, 3H), 1.90–1.40 (m, 6H); δ_{C} (67.8 MHz; CDCl₃): 57.3 (2C), 49.7 (2C), 47.6 (2C), 40.3 (1C), 25.7 (3C, coincidental resonances); IR (liquid film): 3275, 2930, 2800, 1640, 1470, 1440, 1140, 1060 cm⁻¹.

5-Methyl-1,5,9-triazabicyclo[7.3.1]tridecane, **1**

Method A. Lithium aluminium hydride (228 mg) was added to a stirred suspension of the amidinium salt, **6**, (646 mg) in dry THF (10 cm³), and the reaction stirred overnight under nitrogen. Water (0.3 cm³) was added dropwise, followed by 15% sodium hydroxide (0.3 cm³) and water (0.6 cm³). The reaction mixture was stirred for 1 h at room temperature, filtered, and the filter cake washed with THF (10 cm³). The filtrate and washings were combined and the solvent removed under reduced pressure to obtain a yellow oil which was Kugelrohr distilled (80 °C, 0.4 Torr) to yield a clear oil (260 mg, 66.0%) [Found (EI): M⁺, 197.1883. C₁₁H₂₃N₃ requires 197.1892]; δ_{H} (400 MHz; CDCl₃): 5.04 (d, 1H, $J = 11.0$ Hz), 3.97 (d, 1H, $J = 11.0$ Hz), 2.87–2.78 (m, 4H), 2.71–2.61 (m, 4H), 2.49 (ddd, 2H, $J = 12.6, 7.0, 2.8$ Hz), 2.35 (ddd, 2H, $J = 12.9, 8.1, 2.8$ Hz), 2.21 (s, 3H), 2.15 (dtt, 1H, $J = 13.0, 12.6, 5.0$ Hz), 1.77 (m, 4H), 1.55 (m, 4H), 1.18 (dtt, 1H, $J = 13.1, \sim 1.7, \sim 1.7$ Hz); δ_{C} (67.8 MHz; CDCl₃): 70.71 (1C), 56.91 (2C), 53.48 (2C), 53.10 (2C), 43.76 (1C), 28.76 (2C), 21.63 (1C); IR (liquid film): 2940, 2840, 2790, 1450, 1350, 1255, 1205, 1170, 1120, 1040, 935, 785 cm⁻¹.

Method B. Methyl triamine **7** (555 mg) and 37% aqueous formaldehyde solution (0.25 cm³) were refluxed in freshly distilled toluene (60 cm³) using a Dean and Stark apparatus for 3.5 h. The solvent was evaporated to give an orange oil which was Kugelrohr distilled (85 °C, 0.05 Torr) to yield a clear oil (490 mg, 82.9%).

Preparation of 5-methyl-1,5,9-triazabicyclo[7.3.1]tridecane hydrogen picrate, 2·C₆H₂N₃O₇

The picrate salt of **2** was made by reaction of **1** with picric acid in EtOH, and yellow crystals suitable for structure determination were grown by slow diffusion of Et₂O into EtOH solutions of 2·C₆H₂N₃O₇ at room temperature; δ_{H} (270 MHz; CDCl₃): 12.82 (broad, 1H, NH), 4.51 (d, 1H, $J = 12.5$ Hz), 3.71 (d, 1H, $J = 12.5$ Hz), 3.4–1.7 (17H), 2.57 (3H, CH₃), 1.56 (d, 1H, $J = 14$ Hz).

Preparation of 1,4,8,11-tetraazatricyclo[9.3.1.1^{4,8}]hexadecane hydrogen perchlorate, 4·ClO₄

The perchlorate salt of **4** was recrystallised from acetonitrile-ether, and crystals for structure determination were then grown by vapour diffusion of ether into an acetonitrile solution.

Preparation of 1,4,8,11-tetraazatricyclo[9.3.1.1^{4,8}]hexadecane bistrifluoroacetate, 5·2CF₃CO₂

Crystals of 5·2CF₃CO₂ were obtained accidentally during attempts to grow crystals of the monotrifluoroacetate by

Table 1 Structure analyses

Compound	2 ·C ₆ H ₂ N ₃ O ₇	4 ·ClO ₄	5 ·2CF ₃ CO ₂
Formula	C ₁₇ H ₂₆ N ₆ O ₇	C ₁₂ H ₂₅ ClN ₄ O ₄	C ₁₆ H ₂₆ F ₆ O ₄ N ₄
<i>M</i>	426.4	324.8	452.4
Crystal system	Monoclinic	Monoclinic	Monoclinic
Space group (No.)	<i>P</i> 2 ₁ / <i>n</i> (No. 14)	<i>P</i> 2 ₁ / <i>c</i> (No. 14)	<i>P</i> 2 ₁ / <i>c</i> (No. 14)
<i>a</i> /Å	13.098(3)	25.058(5)	7.9210(8)
<i>b</i> /Å	7.196(3)	7.726(2)	15.441(1)
<i>c</i> /Å	21.220(9)	16.163(3)	8.069(1)
β /°	94.29(3)	92.43(2)	93.46(1)
<i>U</i> /Å ³	1994.5(14)	3126.3(10)	985.1(2)
<i>T</i> /K	295	295	295
<i>Z</i>	4	8	2
μ (Mo-K α)/cm ⁻¹	1.05	2.6	1.4
Total data	4004	6187	2614
Unique data	3517	5539	2179
<i>R</i> 1	0.058	0.066	0.045
<i>R</i> _w	0.052	0.071	0.067

vapour diffusion of ether into solutions of **4** treated with trifluoroacetic acid in acetonitrile.

Structural determinations

X-Ray diffraction measurements were made using Nicolet four-circle P3m diffractometers on single crystals mounted in thin-walled glass capillaries. Cell dimensions for each analysis were determined from the setting angle values of 25 centred reflections. Details of the structural analyses are given in Table 1 and the Supplementary Material.† For each structure analysis intensity data were collected by $\omega/2\theta$ scans for unique portions of reciprocal space and corrected for Lorentz, polarisation, and long-term intensity fluctuations on the basis of the intensities of three check reflections repeatedly measured during data collection. No corrections for X-ray absorption effects were applied. Only those reflections with pre-scan counts above a low threshold of 20 cs⁻¹ and having $2\theta > 40^\circ$ were measured for **2**·C₆H₂N₃O₇. The structures were solved by direct and difference Fourier methods, and refined by least-squares against *F*. For **4**·ClO₄ there are two formula units per asymmetric unit, each of the perchlorate ions showed a two-fold disorder corresponding to two orientations being adopted. Their occupancies were refined to 0.11(1) [for O(2'-4')] and 0.89(1) [for O(2'-4)], and 0.27(1) [for O(5'-8')] and 0.73(1) [for O(5'-8')]. The dication **5** has crystallographically-imposed $\bar{1}$ symmetry.

All non-hydrogen atoms were assigned anisotropic displacement parameters with the exception of the low occupancy oxygen atoms of **4**·ClO₄. All carbon-bound hydrogen atoms were constrained to ideal geometries (with C–H = 0.96 Å) and no positional constraints were applied to the nitrogen-bound hydrogens. All hydrogen atoms of **4**·ClO₄ were assigned fixed isotropic displacement parameters; in **5**·2CF₃CO₂ and **2**·C₆H₂N₃O₇, hydrogen isotropic displacement parameters were refined in groups such that all methylene (or aryl, methyl or *N*-bonded) hydrogens had the same parameter value.

Final difference syntheses showed no chemically significant features, the largest being close to the anion atoms. Refinements converged smoothly to residuals given in the Supplementary Material. All calculations were made with programs of the SHELXTL¹⁹ system as implemented on a Nicolet R3m/E structure determination system. Complex neutral-atom scattering factors were taken from the International Tables for X-ray Crystallography.³⁰

† Full crystallographic details, excluding structure factor tables, have been deposited at the Cambridge Crystallographic Data Centre (CCDC). For details of the deposition scheme, see 'Instructions for Authors', *J. Chem. Soc., Perkin Trans. 2*, available via the RSC web page (<http://www.rsc.org/authors>). Any request to the CCDC for this material should quote the full literature citation and the reference number 188/153.

NMR studies of the protonation of 5-methyl-1,5,9-triazabicyclo[7.3.1]tridecane, **1**

Protonation of **1** by CF₃CO₂H in d₆-DMSO was monitored using ¹³C NMR on addition of known aliquots of acid. Addition of < 1 equivalent of CF₃CO₂H to **1** caused broadening of the signals, due to fast intermediate exchange between protonated and unprotonated molecules. Addition of 1 equivalent of CF₃CO₂H gave a spectrum with 7 sharp major signals, corresponding to an averaged spectrum for **2** (fast interconversion of conformers). In addition to the 7 major signals, at least 16 minor signals were observed (*i.e.* at least two other species were present).

Addition of 1.5 equivalents of CF₃CO₂H gave a spectrum with a total of 18 signals, 7 signals for the major and 11 for a minor species in an ~3:1 ratio. Signals for the major species occur at 68.25 (aminal C), 53.62 (broadened), 51.26, 49.02 (broadened), 42.33 (CH₃), 20.32 (broadened), and 19.33 ppm. Signals for the minor species were observed at 75.44 (aminal C), 62.15, 52.38, 50.84, 50.63, 47.22, 45.67, 41.33, 19.84, 18.89, and 18.60 (all sharp). At 2 equivalents of CF₃CO₂H, the spectrum was similar but the ratio of the two species was now ~1:1, the lines at 53.64 and 47.55 were significantly dynamically broadened, and the line at 51.51 was also slightly broadened. At 2.5 equivalents of acid, the two signals previously significantly broadened had disappeared into the baseline and the signal which had previously been slightly broadened was now very broad. Further addition of CF₃CO₂H caused no significant change in the spectra. In neat CF₃CO₂H, **1** gave a ¹³C NMR spectrum with 22 signals, 8 of which were strongly dynamically broadened. The fast interconversion process previously observed for the major species had been slowed sufficiently in neat CF₃CO₂H to give a set of 11 signals, although 8 of these signals were still broad indicating that only intermediate exchange was reached.

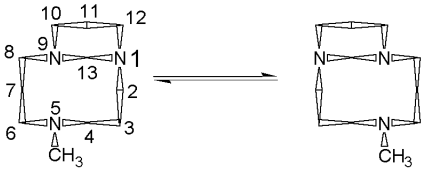
Finally, dissolution of **1** or **2** in neat CF₃SO₃H gave a ¹³C spectrum with signals at 172.51, 56.80, 56.44, 42.76 (double intensity, accidental degeneracy), 42.31, 41.93, 20.49, 19.78, and 15.79 ppm.

Calculations

Molecular mechanics calculations were carried out using Macromodel 5.5.²¹ MM2*, a Macromodel modification of Allinger's MM2 force field,²² and AMBER*, a Macromodel modification of Kollman's AMBER all-atom force field,²³ were employed, the former having the most reliable parametrisation for free amines/aminals (AMBER* has low quality generalized C–N–C bending parameters) and the latter being the only Macromodel force field parametrised for ammonium ions. AMBER* calculations utilized the Lennard-Jones H-bond treatment of Ferguson and Kollman.²⁴ Calculations employed constant dielectric electrostatics [relative permittivity (dielectric constant) = 1] unless otherwise stated; extended nonbonded cutoff distances were used in AMBER* calculations. The Generalized Born/Solvent Accessibility (GB/SA)²⁵ CHCl₃ solvation model was generally used. All searches of conformational space employed the usage-directed Monte Carlo Multiple Minimum (MCMM) method.²⁶ In each case, 10 000 MC steps were carried out and all low energy conformers were found at least 30 times (typically many more), indicative of good search convergence. Global minima and selected additional conformations were checked to ensure that they were true minima rather than saddle points.

PM3²⁷ calculations were carried out using CSMopac (Mopac93, Fujitsu Ltd.). Density functional calculations were carried out by the perturbative Becke–Perdew method implemented in Spartan V5.0,²⁸ using the DN** numerical basis set, which is similar to 6-31G**.

All *ab initio* calculations were performed using GAUSSIAN-92 or GAUSSIAN94 on an IBM RS6000/3AT computer

Table 2 ^{13}C DNMR data^a for 5-methyl-1,5,9-triazabicyclo[7.3.1]tridecane, **1**


$T/^\circ\text{C}$	C_{13}	NCH_2 ($\text{C}_{2,8}$; $\text{C}_{4,6}$; $\text{C}_{10,12}$)			Me	$\text{C}_{3,7}$	C_{11}
+20	71.77	57.66	54.02	53.94	44.10	29.47	22.95
-30	71.54	57.31	53.97	— ^b	44.24	29.29	22.44
-55	71.58	57.26	54.09	— ^b	44.36	29.37	22.20 ^c
-60	71.68	57.05	54.27 ^c	— ^b	44.40	29.43	22.17 ^c
-65	71.52	57.14	54.05 ^c	— ^b	44.39	29.27 ^c	21.93 ^c
-70	71.52	57.10	54.03 ^c	— ^b	44.40	~29.3 ^c	21.79 ^c
-75	71.52	57.05 ^c	54.09 ^c	~56 ^c	44.40	~29.2 ^c	21.02 ^c
-80	71.52	~52 ^c 56.97 ^c	54.13 ^c	~56 ^c 51.37 ^c	44.37 ^c	^d	20.97 ^c
-85	71.58	57.32 ^c 56.62 ^e	54.27 ^c 53.23 ^c	56.64 ^e 51.42 ^c	44.29 ^c	^d ~29 ^c	20.93 ^c
-90	71.64 ^c	57.45 ^c 56.48 ^e	54.28 ^c 53.23 ^c	56.48 ^e 51.27 ^c	44.26 ^c	^d 28.86 ^c	20.73 ^c
-95	71.85 ^c	57.60 ^c 56.42 ^c	54.35 ^c 53.35 ^c	56.68 ^c 51.31 ^c	44.27 ^c	^d 28.92 ^c	20.78 ^c

^a Solvent d_6 -acetone (0.5 ml) containing 100 mg of triamine, δ downfield of TMS. ^b Obscured by overlapping signal. ^c Significantly broadened. ^d Buried under d_6 -acetone multiplet. ^e Mutual overlap.

running AIX 4.2.^{29,30} Standard Pople-style basis sets were used as implemented in Gaussian. The extended basis set tz(2d,2p)++ is the Dunning–Hay triple- ζ basis set³¹ augmented with two sets of polarization functions on carbon (exp = 0.375, 1.5), nitrogen (exp = 0.45, 1.8) and hydrogen (exp = 0.55, 2.20) with the addition of a single uncontracted p -type function on heavy atoms and a single uncontracted s -type function on hydrogen according to the recommendations of Clark *et al.*³² All correlation methods were used as implemented in GAUSSIAN94.³⁰ Natural Bond Orbital calculations³³ were done using Version 4.0 of Weinhold and co-workers' NBO code as implemented in GAUSSIAN94. Deletion-optimizations within the NBO framework were performed as previously described.^{8,35}

Results and discussion

Preparations and structures of 5-methyl-1,5,9-triazabicyclo[7.3.1]tridecane and 1,4,8,11-tetraazatricyclo[9.3.1.1^{4,8}]-hexadecane

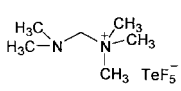
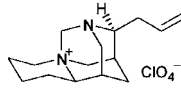
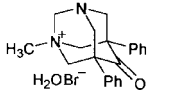
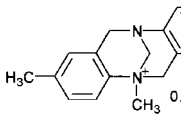
5-Methyl-1,5,9-triazabicyclo[7.3.1]tridecane, **1**, can be readily prepared from 1,5,9-triazatricyclo[7.3.1.0^{5,12}]tridecane by alkylation with iodomethane, followed by reduction of the amidinium salt, **6**, by LiAlH_4 . Alternatively, **6** can be hydrolysed to the monocyclic triamine **7** and then reacted with formaldehyde to produce **1** (Scheme 1).

5-Methyl-1,5,9-triazabicyclo[7.3.1]tridecane is conformationally related to 1,5-diazabicyclo[7.3.1]tridecane, for which the dominant conformation has been shown¹⁵ to be a BCB or [2323] conformation³⁶ for the ten-membered ring with the six-membered ring fused on in an *equatorial,axial* (*eq,ax*) fashion so that one lone pair is inside, and one outside (representations of this and other conformations according to Dale's conventions³⁶ are shown alongside the normal structural formulae). A similar conformation is likely for **1**, even though this puts the lone pairs of the N-Me and one aminal nitrogen atom in direct transannular interaction. MCOMM searches of the conformational space of **1** using MM2* and AMBER* both gave this

eq,ax-[2323] conformation as the global minimum. The MM2* search found a gap between the global minimum and next higher energy conformation of 21.0 kJ mol⁻¹ and all 44 unique conformers within 50 kJ mol⁻¹ to be *eq,ax* at the hexahydropyrimidine ring. In comparison, the AMBER* search found 27 additional conformers within 20 kJ mol⁻¹ of the global minimum, two within 4 kJ mol⁻¹, and an *ax,ax* (*out,out*) conformer only 11.0 kJ mol⁻¹ above the global minimum. Despite the quantitative disagreement between the force field results, which we attribute at least in part to the low quality C–N–C bending parameters in AMBER*, the results point qualitatively to dominance of *eq,ax* conformers and the likelihood that the diamond-lattice [2323] conformer is the global minimum and is certainly significantly populated. The 400 MHz ¹H NMR spectrum of **1** at room temperature exhibits a dynamically unbroadened AB spectrum ($\Delta\delta = 1.07$ ppm; $J = 11.0$ Hz) for the aminal protons. This shows that the process which passes the aminal methylene through the ten-membered ring with net inversion of both rings is slow on the NMR timescale ($\Delta G_{296}^\ddagger > 63.4$ kJ mol⁻¹). The results of a low temperature ¹³C DNMR study of **1** are shown in Table 2. Four of the seven resonances at room temperature decoalesced on cooling into pairs of lines. The remaining three resonances (C_{11} , C_{13} , and the methyl carbon) remained dynamically unbroadened, although at the lowest temperatures the signals were anisotropically broadened. These results are consistent with the slowing of enantiomerisation of *eq,ax*-[2323] **1**, the dynamic process involving sequential inversion of the two aminal nitrogens and torsional changes (not ring inversion) in the ten-membered ring. Application of the coalescence temperature (T_c) approximation to the decoalescence processes of the 57.66, 54.02, and 53.94 resonances gives $\Delta G_{193 \pm 2}^\ddagger = 38.4 \pm 0.5$, $\Delta G_{193 \pm 2}^\ddagger = 38.5 \pm 0.5$, and $\Delta G_{208 \pm 2}^\ddagger = 38.7 \pm 0.5$ kJ mol⁻¹ respectively, in excellent agreement with the results previously obtained for the enantiomerisation of 1,5-diazabicyclo[7.3.1]tridecane.¹⁵

1,4,8,11-Tetraazatricyclo[9.3.1.1^{4,8}]hexadecane **3** was prepared by reaction of cyclam with formaldehyde.¹⁵ The preferred diamond lattice conformation of this bis-formal has been established by X-ray structure determination¹⁴ and NMR studies.¹⁵

Table 3 Bond lengths (Å) in $R_2NCHRNR_3^+$ ions from the Cambridge Crystallographic Database

	$R_2N-CH_2N^+R_3$	Other C–N	$R_2NH_2C-N^+R_3$	Other C–N ⁺	Reference
 <p>(Dimethylaminomethyl)trimethylammonium pentafluorotellurate(IV)</p>	1.431	1.469, 1.472	1.550	1.492, 1.494, 1.498	46
 <p>Anhydro-<i>N</i>-hydroxymethyl deoxyangustifoline perchlorate</p>	1.416	1.470, 1.497	1.541	1.504, 1.528, 1.529	47
 <p>5,7-Diphenyl-1-methylazonia-3-azaadamantan-6-one bromide monohydrate</p>	1.415	1.461, 1.465	1.539	1.498, 1.502, 1.515	48
 <p>1,5,13-Trimethyl-1-azonia-9-azatetracyclo[7.7.1.0^{2,7}.0^{10,15}]heptadeca-2,4,6,10,12,14-hexaene iodide dioxane clathrate</p>	1.424	1/436 (N–Ar), 1.464	1.545	1.493, 1.501, 1.503	49

As we shall show below, the conformation is changed completely by mono-protonation, but is restored on di-protonation.

Experimental evidence for structural anomeric effects in aminals $R_2NCHRNR_2$ and in $R_2NCHRNR_3^+$ ions

Before discussing hydrogen-bonded systems, we briefly consider existing evidence for structural anomeric effects in (a) neutral aminals and (b) in $R_2NCHRNR_3^+$ ions where one nitrogen atom carries a full positive charge. There is little evidence for bond shortening and lengthening in aminals, even where the conformation is ideally set up, as in *equatorial,axial*-hexahydropyrimidines.¹⁴ A search of the Cambridge Crystallographic Database for simple aminals of general structure $RR'NCH_2NR''R'''$ (R, R', R'', R''' saturated) gave 12 structures^{14,37} after elimination of compounds having additional interacting functional groups. Comparison of the reported aminal C–N bond lengths and associated standard uncertainty values (s.u.; formerly known as e.s.d.) showed that most of the bond lengths are within 3 s.u.'s of one another, irrespective of lp–N–C–N torsion angle. The effect is simply below the noise level of the measurement method.³⁸ In the few cases where C–N bond lengths appear to be significantly different, the difference runs counter to expectation^{37(e),37(i)} and/or may be attributed to steric effects.^{37(i),37(k)} Thus, the experimental evidence for a structural anomeric effect in simple aminals is not strong at this point.

The evidence for structural anomeric effects in $R_2NCHRNR_3^+$ ions is much more convincing; R_2N-CH bonds are shortened and $HRC-NR_3^+$ bonds lengthened. A search of the Cambridge Crystallographic Database for $R_2NCHRNR_3^+$ ions turned up over 30 structures, but the majority of these were based on hexamethylenetetramine (1,3,5,7-tetraazaadamantane), where several amino groups can potentially donate electrons towards the ammonium centre, so that any structural

effects are diluted. These structures were not considered further. Systems involving potential π -bonding to the amino group were also rejected. Data for the four most relevant structures are summarised in Table 3, and these do produce clear evidence for the operation of a structural anomeric effect in the normal direction. In each case, the bond between the quaternary nitrogen atoms and the aminal carbon is lengthened compared to standard C–N⁺ bonds,³⁹ (and is the longest bond to that nitrogen), while the bond from the aminal carbon to the tertiary nitrogen is shortened (and is shorter than other bonds to that nitrogen). The structural anomeric effect should be strongly dependent on the lp–N–C–N⁺ torsion angle. In a subsequent paper, we will demonstrate how strong structural anomeric effects in tricyclic $R_2NCHRNR_3^+$ ions depend on the differences in strain between closed and open species and on the lp–N–C–N⁺ torsion angle.⁴⁰ In all but one of the structures shown in Table 3, the lone pair is essentially antiperiplanar to the C–N⁺ bond which is lengthened, but in the acyclic example, the lp–N–C–N⁺ torsion angle is 0°, undoubtedly due to the avoidance of g^+g^- interactions. The latter structure is interesting in another respect, because the tertiary nitrogen is significantly flattened, the sum of the C–N–C angles being 338.2°.

Structural evidence for anomeric effects in ions 2, 4, and 5

Perspective views of the molecular structures of cations **2**, **4**, and **5** are given in Figs. 2–4. Tables 4–6 list the important bond lengths and angles for these structures. The crystal structures of **2**· $C_6H_2N_3O_7$ and **4**· ClO_4 consist of isolated anions and cations separated by normal distances and in both there are intramolecular N–H···N hydrogen bonds (see below). In **5**· $2CF_3CO_2$, the two independent dicationic sites are sited about crystallographic inversion centres in the crystal and therefore show strict C_i site symmetry. There are N–H···O hydrogen bonds [N(3)···O(1') 2.676 Å where O(1') is related to O(1) by the

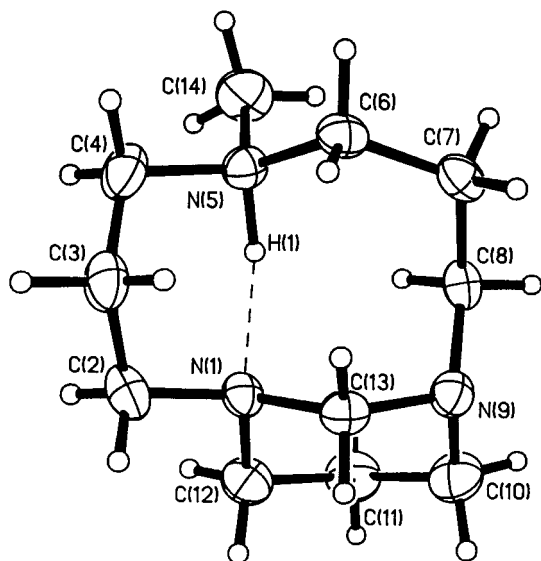


Fig. 2 Molecular structure of **2** showing labelling scheme.

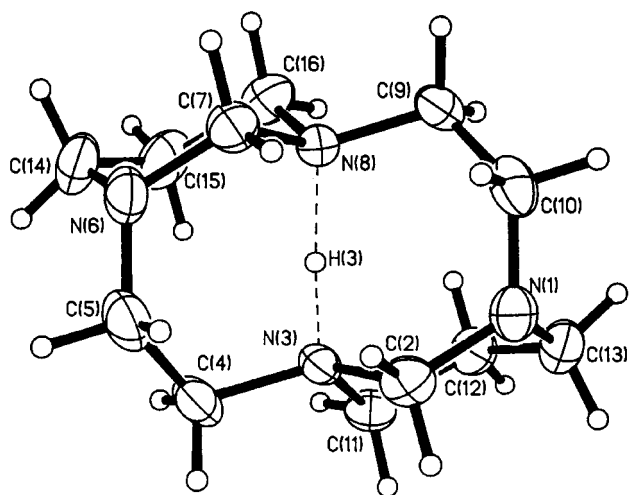


Fig. 3 Molecular structure of the first of two independent cations **4** showing labelling scheme.

symmetry operation $x, 1.5 - y, 0.5 + z$] between cations and anions.

Intramolecularly hydrogen-bonded ions from derivatives of 1,3-diaminopropane usually adopt conformations [see Fig. 5(a)] such that the C_3N_2H unit forms a chair-like six-membered ring, the hydrogen atom occupying the place of one carbon atom in cyclohexane so that the hydrogen bond is strongly bent. Examples are inside-protonated 1,8-diazabicyclo[6.4.3]penta-decane picrate, **8a**, and inside-protonated 1,8-diazabicyclo-[6.5.3]hexadecane picrate, **8b**, where the $N-H \cdots N$ angles were found,^{41,42} to be 155 and 154° respectively. On the other hand, intramolecularly hydrogen bonded ions from derivatives of 1,4-diaminobutane usually adopt conformations such that the C_4N_2 unit forms a chair-like structure, the entire $N-H \cdots N$ bond (now almost linear) taking the place of a $C-C$ bond in cyclohexane [see Fig. 5(b)]. Good examples are the structure of the monoprotonated ion **9** from 1,6-dimethyl-1,6-diazacyclo-decane,⁴³ and of inside-protonated 1,6-diazabicyclo[4.4.4]-tetradecane.⁴⁴ Thus the structure of **2** might be expected to be based on the diamond lattice structure for tricyclo[7.3.1.1^{1,5}]-tetradecane **10**, while that for **4** should relate to the diamond lattice structure for tetracyclo[9.3.1.1^{1,8}.1^{4,8}]-hexadecane **11**, the $N-H \cdots N$ unit occupying the position of the central $C-C$ bond of the latter.

These expectations are nicely borne out by the structures shown in Fig. 2 and 3. In the picrate salt $2 \cdot C_6H_2N_3O_7$, the

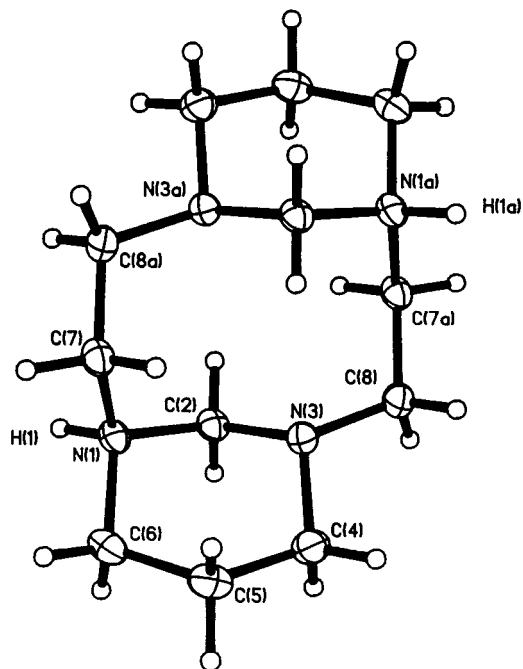


Fig. 4 Molecular structure of **5** showing labelling scheme.

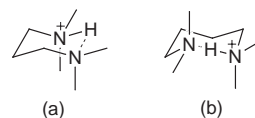
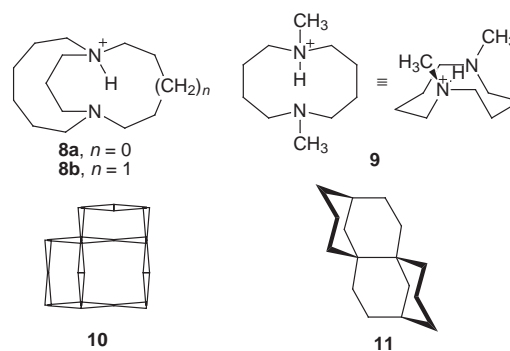


Fig. 5 Relationship of intramolecular hydrogen bonded structures from 1,3-diaminopropanes and 1,4-diaminobutanes to chair cyclohexane.



cation adopts the same diamond lattice conformation discussed above for **1**, but the ten-membered ring is distorted from the ideal [2323] conformation in an interesting way, with the $N-H \cdots N$ unit rotating inwards to provide a more linear hydrogen bond. This allows the adjacent methylene groups which are involved in a transannular non-bonded interaction to rotate away from each other. In **2** the $N-H \cdots N$ system is relatively asymmetric and remarkably close to those seen in **8a** and **8b**. As shown in Table 4, this similarity extends to the differences in $N-C$ bond lengths at $N(1)$ and $N(5)$. The hydrogen bond in **2** is probably relatively weak both because the bond is quite bent and because the amino nitrogen is more basic than the aminal nitrogen atoms, but it nevertheless induces a small, but significant, structural anomeric effect in the aminal portion of the molecule. The $lp-N(9)-C(13)-N(1)$ torsion angle in **2** is 174.7°, close to the ideal antiperiplanar situation which should maximise any structural anomeric effect. In fact, the length of the $N(1)-C(13)$ aminal bond is not significantly increased compared with the other $N-C$ bonds to this atom, but the length of the $C(13)-N(9)$ bond is decreased (incipient double bonding) to 1.440(4), 0.026/0.030 Å (> 5 s.u.) shorter than $C(8)-N(9)/$

Table 4 Selected bond lengths (Å) and angles (°) for 5-methyl-1,5,9-triazabicyclo[7.3.1]tridecane hydrogen picrate, 2·C₆H₂N₃O₇, and corresponding structural data for **8a** and **8b**

	X-ray data for 2·C ₆ H ₂ N ₃ O ₇	DFT (pBP/DN**) calculation	Data for 8a	Data for 8b
N(1)···N(5)	2.707(5)	2.659	2.663(4)	2.610(5)
N(5)–H(1)	1.04(3)	1.137	0.950(19)	1.19(3)
N(1)···H(1)	1.76(3)	1.601	1.772(21)	1.49(3)
N(1)···H(1)–N(5)	149(3)	152.0	154.8(13)	154(3)
N(1)–C(2)	1.466(4)	1.488	1.491(3)	1.504(5)
N(1)–C(12)	1.475(4)	1.494	1.484(3)	1.495(6)
N(1)–C(13)	1.477(4)	1.501	1.486(3)	1.472(6)
N(9)–C(8)	1.466(4)	1.475		
N(9)–C(10)	1.470(4)	1.483		
N(9)–C(13)	1.440(4)	1.442		
N(5)–C(4)	1.513(5)	1.517	1.506(3)	1.485(6)
N(5)–C(6)	1.494(4)	1.510	1.509(2)	1.516(7)
N(5)–C(14)	1.482(5)	1.492	1.493(2)	1.486(5)
C(2)–N(1)–C(12)	111.5(3)	111.7		
C(2)–N(1)–C(13)	113.2(2)	113.0		
C(12)–N(1)–C(13)	107.6(3)	108.5		
C(4)–N(5)–C(6)	112.7(2)	113.2		
C(4)–N(5)–C(14)	111.5(3)	111.6		
C(6)–N(5)–C(14)	111.8(3)	112.0		
C(8)–N(9)–C(10)	109.8(3)	111.0		
C(8)–N(9)–C(13)	115.3(2)	116.3		
C(10)–N(9)–C(13)	107.8(3)	108.6		
Σ(N–C–N) at <i>out</i> -N	332.9			
lp-N(9)–C(13)–N(1)	174.7°			

Table 5 Selected bond lengths (Å) and angles (°) for 1,4,8,11-tetraazatricyclo[9.3.1.1^{4,8}]hexadecane hydrogen perchlorate, 4·ClO₄ and corresponding structural data for **9**

	X-ray data	DFT (pBP/DN**)	Data for 9
N(3)···N(8)	2.581(6)	2.624	2.600(3)
N(19)···N(24)	2.571(6)		
N(3)–H(3)	1.22(5)	1.186	1.30(5)
N(19)–H(19a)	1.18(4)		
N(8)–H(3)	1.38(5)	1.459	1.30(5)
N(24)–H(19a)	1.40(4)		
N(3)–H(3)–N(8)	165(4)	165.4	169(2)
N(19)–H(19a)–N(24)	171(4)		
N ^{δ+} –C _{aminal} (average)	1.494(6)	1.520	
<i>out</i> -N–C _{aminal} (average)	1.419(6)	1.430	
Non-aminal N ^{δ+} –C (average)	1.475	1.492	1.490
Non-aminal <i>out</i> -N–C (average)	1.456	1.469	
Σ(N–C–N) at <i>out</i> -N	347.0	348.9	
lp-N–C–N (average)	172°		

C(10)–N(9) and 0.022 Å (> 6 combined s.u.) shorter than the corresponding aminal bond in **3** (Table 6). These effects are reproduced well by a density function theory calculation on **2** at the pBP/DN** level, which gave remarkable agreement with the X-ray geometry (Table 4). From this calculation, we see that the HOMO is essentially a lone pair orbital on the *out*-N (the anomeric effect donor atom), which is somewhat delocalised into the N(1)–C(13) bond. The HOMO(–1) orbital is essentially a lone pair orbital on the *in*-N (involved in the transannular hydrogen bond).

The relatively weak hydrogen bonding in 2·C₆H₂N₃O₇ is consistent with the NMR observations of **2** in CDCl₃ solution, where the NH for **2** is observed as a broadened singlet at δ 12.82, compared with 14.62 for **8a** and 13.78 for **8b**.⁴⁵ **2**, like **1** itself, shows a seven line ¹³C NMR spectrum due to dynamic averaging between two enantiomeric conformers or families of conformers. Two mechanisms for this enantiomerisation seem possible (a): inversion of the *out*-nitrogen atom to give an *in, in*-isomer in which the seven-atom bridge is fused *eq, eq* to the hexahydropyrimidine ring, or (b) inversion of the *in*-nitrogen to give an *out, out*-isomer, with *ax, ax* fusion of the seven-atom bridge to the six-membered ring. Mechanism (a) benefits from the fact that the hydrogen bond is never broken, but converted temporarily to a bifurcated H-bond, whereas the intermediates in mechanism (b) involve complete rupture of the hydrogen bond, but involve ring conformations with much less strain. A multiple minimum search using the AMBER* force field in MacroModel located two *in, in*-conformations which were predicted to be lower in energy than the X-ray structure. The global minimum structure, according to AMBER* lacked any symmetry, while the next structure had a plane of symmetry bisecting the bifurcated hydrogen bond. AMBER* generally gives a good account of hydrogen bonding but, as has been previously pointed out, underestimates bond angle bending at nitrogen, and so may be expected to unduly favour *in, in*-conformations. However, when the two *in, in*-conformations located by AMBER* were minimised by density function theory calculation at the pBP/DN** level, they were found to be only 5.6 and 12.3 kJ mol^{–1} above the X-ray *in, out*-structure. We believe that this suggests that mechanism (a) is viable for **2**.

The structural anomeric effect induced by H-bonding in **2** is small, and we wanted to design an ion containing a strengthened hydrogen bond where a larger effect might be induced. Many structural changes which might achieve this can be contemplated, but the “half-protonation point”, where a proton is

shared between two equivalent aminals, seemed a particularly attractive target. We also knew that the hydrogen bond in **9** (a butane-1,4-diamine derivative) was close to linear and probably as strong as could be obtained in a transannular situation. Combining these features led naturally to 1,4,8,11-tetraazatricyclo[9.3.1.1^{4,8}]hexadecane, **3**, although this implied that the molecule would have to undergo a change of conformation from that in the free bisaminal^{14,15} when monoprotonation occurred. This was indeed the case in **4**, and the return to the same conformation as the free base **3** on diprotonation in **5** was a bonus (Fig. 3 and 4). The unit cell was found to contain two independent but similar ions of **4**, each possessing an approximate axis of symmetry (one is illustrated in Fig. 3). The hydrogen bonds in the independent cations **4** are nearly linear and almost symmetrical (see Table 5); the N...N distance and N...H-N⁺ angle are very similar to those reported for **9**,⁴³ and clearly indicate a very strong and nearly symmetrical bond. This is in keeping with the observed IR absorption near 1500 cm⁻¹, and the ¹H NMR absorption at δ 17.1, compared to 15.71 for **9**.⁴⁵ The structural anomeric effect induced by the hydrogen

Table 6 Selected bond lengths (Å) and angles (°) for 1,4,8,11-tetraazatricyclo[9.3.1.1^{4,8}]hexadecane **3** and for its diprotonated ion (**5**·2CF₃CO₂)

	X-ray data for 5 ·2CF ₃ CO ₂	Corresponding structure data for 3	DFT (pBP/DN ¹⁶ **)
N(1)–C(2)	1.503(2)	1.462(2)	1.531
N(1)–C(6)	1.507(2)	1.478(2)	1.538
N(1)–C(7)	1.502(2)	1.473(2)	1.526
N(3)–C(2)	1.441(2)	1.465(2)	1.441
N(3)–C(4)	1.464(2)	1.465(2)	1.483
N(3)–C(8)	1.467(2)	1.471(2)	1.478
Σ (N–C–N) at <i>in</i> -N	336.9	335.1	338.3
lp-N(3)–C(2)–N(1)	49.9		

bond in **4** is indeed markedly greater than that seen in **2**. The lp-N(9)–C(13)–N(1) torsion angle in **4** is 172°, again close to the ideal antiperiplanar situation which should maximise any structural anomeric effect. The average length of the N^{δ+}–C_{aminal} bond (see Table 5) is now marginally larger (0.019 Å) than the average of all the non-aminal N^{δ+}–C bonds in the structure and significantly larger (0.29 Å) than the corresponding aminal bond in **3**. The average length of the *out*-N–C_{aminal} bond in **4** is shortened by 0.037 Å compared to the average of all the non-aminal *out*-N–C bonds and is significantly shorter (0.043 Å) than the corresponding aminal bond in **3** (Table 6). We also note that the sum of the bond angles at the anomeric effect donor atom is 347°, indicating substantial flattening at this atom; for **2** this sum is 332.9°. It is interesting to note that in **4** there is some degree of delocalisation over the entire [N–C–N...H...N–C–N]⁺ system.

¹³C NMR and ¹H NMR spectra of **4** with BF₄⁻, I⁻, or ClO₄⁻ counterions were dynamically broadened at room temperature, and low temperature ¹³C NMR and ¹H NMR spectra were therefore obtained. 1D and 2D ¹H NMR spectra of **4**·ClO₄ were obtained under slow exchange conditions at –20 °C. Table 7 shows the assigned chemical shifts for the protons and coupling constants for one half of the symmetrical molecule. The data for **4** is consistent with the adoption of the same conformation in solution as in the solid-state. In particular, we note that:

a) protons H^{2a}, H^{7b}, and H^{16b} show measurable coupling to the NH whereas their geminal partners do not. H^{2a}, H^{7b}, and H^{16b} are therefore likely to be the protons which are most nearly antiperiplanar to this proton. Note that when an N–H bond has an effective bond order of 0.5 as in this case, couplings to the NH are typically reduced by about one half.

b) protons H^{5a} and H^{7a} show long range W-coupling to H^{16a}. These three protons must therefore all be equatorial in the hexahydropyrimidine ring.

c) the coupling between H^{2a} and H^{3b} is consistent with the X-ray conformation within the N–C–C–N unit.

¹³C DNMR spectra of **4** showed that dynamically-broadened N–C signals decoalesced into pairs of lines with decreasing temperature (slow exchange limit at 0 °C), due to slowing of the

Table 7 Chemical shifts (ppm) and coupling constants (Hz) for **4**·ClO₄

	NH	H ^{2a}	H ^{2b}	H ^{3a}	H ^{3b}	H ^{5a}	H ^{5b}	H ^{6a}	H ^{6b}	H ^{7a}	H ^{7b}	H ^{16a}	H ^{16b}
ppm	17.1	2.63	2.70	3.38	3.14	3.07	3.10	1.80	1.60	3.20	2.95	4.13	3.64
NH		1.2									3.9		4.1
H ^{2a}			13.7	4.4	5.6								
H ^{2b}				12.7	4.4								
H ^{3a}					16.6								
H ^{3b}													
H ^{5a}							14.6	5.4				~1.5	
H ^{5b}								12.7					
H ^{6a}									14.4	5.4	12.7		
H ^{6b}											5.4		
H ^{7a}											12.0	~1.5	
H ^{7b}													
H ^{16a}													12.7
H ^{16b}													

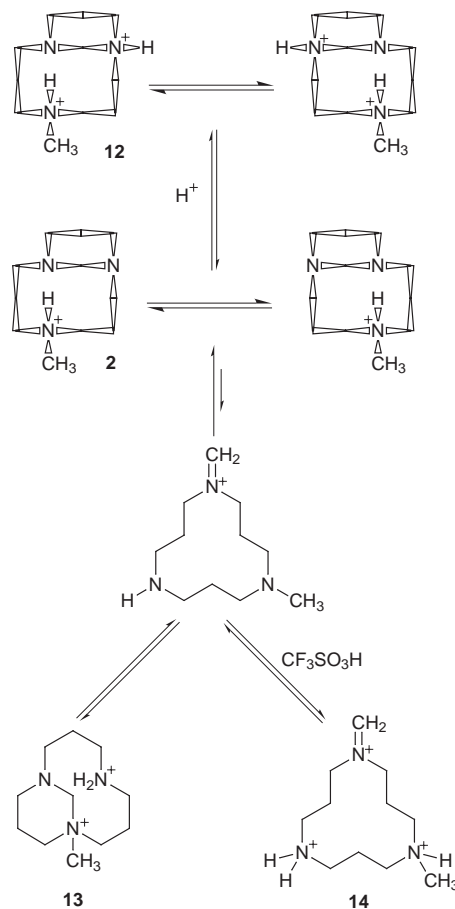
enantiomerisation process. Calculation of the energy barrier for enantiomerisation of **4** using the coalescence temperature approximation gives $\Delta G^\ddagger = 43.5 \text{ kJ mol}^{-1}$. The barrier is therefore higher than the topomerisation barrier for **3** itself ($\Delta G^\ddagger = 38 \text{ kJ mol}^{-1}$). In the case of **4**, enantiomerisation must involve net inversion of all four nitrogen atoms and proton transfer such that the $\text{N} \cdots \text{H}-\text{N}^+$ unit is transferred from one pair of nitrogens to the other. Enantiomerisation could involve initial inversion of the *out*-nitrogen atom to give an *eq,eq,eq,ax*-conformer containing a bifurcated hydrogen bond as discussed for **2** above, but an AMBER* search of the conformational space of **4** did not find an *eq,eq,eq,ax*-conformer within 50 kJ mol^{-1} of the global minimum, and so this mechanism does not seem likely. The AMBER* global minimum was found to correspond to the X-ray geometry and this was 9.9 kJ mol^{-1} lower in steric energy than the next conformation. The alternative of breaking the hydrogen bond first followed by inversion of the *in*-nitrogen atom to an *eq,ax,ax,ax*-conformer is probably the most economical process.

The structure of the bis(trifluoroacetate) of **5** is also interesting (Fig. 4 and Table 6). The general conformation of the dication now reverts to that for **3**, with the NH protons involved in hydrogen bonding to the CF_3CO_2^- counterions. As was seen for **2** and **4**, the N–C bond lengths to the protonated nitrogen are lengthened compared with those to the *in*-N. The $\text{lp}-\text{N}-\text{C}-\text{N}^+$ torsion angle is close to *gauche* (49.9°), and so the overlap required for the anomeric effect is relatively small. There is no significant difference between the three C–N bonds to the protonated nitrogen atoms, but the bond between the aminal carbon and the non-protonated nitrogen is about 0.02 Å shorter than the two other C–N bonds to that nitrogen atom. This bond shortening can be due to the structural anomeric effect, but may be partly due to an inductive effect from the protonated nitrogen which should be independent of torsion angle. It is reproduced well by the DFT calculation (Table 6).

In summary, the four-coordinated aminal nitrogens in **2**, **4**, and **5** show longer N–C distances to the aminal carbon than do the three-coordinate nitrogens; the $\text{N}^{\delta+}-\text{C}$ distances average 1.494(6) Å in **4**, and are 1.477(4) and 1.503(2) Å in **2** and **5**, *cf.* the N(3-coord)–C distances which average 1.419(6) Å in **4** and are 1.441(2) and 1.440(4) Å in **2** and **5** respectively. The N–C bond length differences [$\Delta = d(\text{N}^{\delta+}-\text{C}) - d(\text{N}(3\text{-coord})-\text{C})$] are largest in **4** (0.075 Å), are intermediate in **5** (0.062 Å), and are smallest (0.037 Å) in **2**.

NMR studies of the further protonation of **2**

Further protonation of **2** by excess acid did not produce salts which were suitable for structure determinations, but some interesting observations were made by NMR. Addition of excess $\text{CF}_3\text{CO}_2\text{H}$ to solutions of **2** in d_6 -DMSO produces dications, which analyses of ^{13}C NMR spectra show to be an approximately 1:1 mixture of two species. One ion is clearly related to **2** and we suggest protonation of the outside aminal nitrogen atom (not involved in the intramolecular hydrogen bond) to give **12** (Scheme 2). An AMBER* conformational search (GB/SA CHCl_3) of **12** gave an *eq,ax*-[28]conformer as global minimum, with *eq,ax*-[2323] as the next conformer. Reminimisation of conformers (no solvent) using either distance dependent dielectric electrostatics or constant dielectric electrostatics with relative permittivity for DMSO (46.7) gave *eq,ax*-[2323] as the global minimum of this highly polar species. At low acid concentrations, **12** is in rapid dynamic equilibrium with **2** (seven ^{13}C signals). With increasing acid concentration, the proportion of **12** increases with concomitant slowing of enantiomerisation. In neat $\text{CF}_3\text{CO}_2\text{H}$, a slow intermediate exchange spectrum for **12** is observed (11 lines, eight still broadened). A second species shows 11 sharp lines throughout and so is clearly unable to undergo any rapid averaging by conformational and/or proton transfer processes like **12**. A further

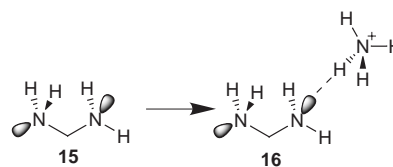


Scheme 2

clue to the nature of this species came from dissolution of **1** or **2** in neat $\text{CF}_3\text{SO}_3\text{H}$, when a ^{13}C spectrum containing ten signals was obtained (one accidental degeneracy). The signal due to the aminal carbon atom at *ca.* 65–80 ppm was then replaced by a signal at 172.51 ppm, suggesting the formation of the monocyclic trication **14** with a $\text{H}_2\text{C}=\text{N}^+$ group. We therefore propose that the second species is **13**, obtained from **12** *via* ring opening to a monocyclic iminium ion (Scheme 2); this reaction is slow on the NMR time scale and **13** shows the expected eleven ^{13}C signals. It is expected that **13** should adopt the same type of *eq,ax*-[2323] conformer as **12**. PM3 geometry optimisations of *eq,ax*-[2323] conformers of **12** and **13** gave almost identical energies, consistent with the experimentally observed equilibrium of ~1:1.

Ab initio calculations on model systems

In order to probe the stereoelectronic nature of the interaction of an aminal nitrogen with a protonated amine, a series of *ab initio* calculations on the simplest model systems were performed. Specifically, geometry optimization of diaminomethane **15** (Scheme 3) in the absence and presence of an



Scheme 3

ammonium ion were performed with the orientation of the lone-pairs in **15** corresponding to those found in the macrocyclic ions **2** and **4**. Calculations were performed using the 6-31+G* basis set of Pople and an augmented form of the

Dunning–Hay triple- ζ basis set (see the Experimental section for details). Geometry optimizations were performed at the SCF and MP2 levels of theory with both basis sets to insure no model dependence.

Optimisation of **15** in the gas phase reveals CN bond lengths of 1.4581/1.4713 Å and 1.4426/1.4498 Å and a NCN bond angle of 112.95/112.93° at RHF/6-31+G* and MP2/6-31+G*, respectively. The bond length changes are quite small, in accord with the lack of evidence for significant structural anomeric effects in aminals discussed earlier, but they are in the expected direction for a single $n(\text{N}) \rightarrow \sigma_{\text{CN}}^*$ interaction. This conformation is similar to that observed in β -glycosides, in which anomeric stabilization has been shown to be a major determinant of structure.^{1–7} The observed changes in the CN bond lengths upon inclusion of electron correlation at the MP2 level is consistent with previous work, and is characteristic of anomeric-type stereoelectronic interactions.^{8,35}

Coordination of the ammonium ion with **15** takes place at the nitrogen lone pair not involved in the internal $n(\text{N}) \rightarrow \sigma_{\text{CN}}^*$ anomeric interaction and specifically involves a formal charge-transfer interaction of the lone pair with the σ_{NH}^* centered on the ammonium ion. In this conformation, the internal $n(\text{N}) \rightarrow \sigma_{\text{CN}}^*$ donor–acceptor interaction is strengthened in the complex **16** compared to that observed for **15** (Scheme 3). This effect can be seen in the two internal CN bond lengths which change considerably upon interaction with the ammonium ion ($\Delta r_{\text{CN}} = 0.0266$ and -0.0075 Å at RHF/6-31+G*; $\Delta r_{\text{CN}} = 0.0289$ and -0.0092 Å at MP2/6-31+G*). The shortening of the CN bond involved in the original anomeric interaction suggests that the acceptor strength of the σ_{CN}^* is increased. This presumably results from the loss of electron density at the second nitrogen when the lone pair becomes involved in the intermolecular charge transfer interactions with the ammonium ion, *i.e.* an $n(\text{N}) \rightarrow \sigma_{\text{NH}}^*$ interaction from the second nitrogen lone pair. The transfer of electron density makes the nitrogen more electropositive, thereby forcing internal charge transfer, the $n(\text{N}) \rightarrow \sigma_{\text{CN}}^*$ interaction, to compensate. Concomitant changes in the internal NCN bond angle of the amina are also observed ($\Delta a_{\text{NCN}} = 0.96$ and 1.3° at RHF/6-31+G* and MP2/6-31+G*, respectively), consistent with an increase in the strength of the internal $n(\text{N}) \rightarrow \sigma_{\text{CN}}^*$ interactions.

Taken together, these calculated changes in geometry are consistent with a cooperative network of charge-transfer or hyperconjugative interactions that extend from the lone pair involved in the original $n(\text{N}) \rightarrow \sigma_{\text{CN}}^*$ interaction to the σ_{NH}^* centered on the coordinating ammonium ion through a critical $n(\text{N}) \rightarrow \sigma_{\text{NH}}^*$ interaction centered at the second nitrogen.

The Natural Bond Orbital (NBO) method of Weinhold and co-workers is a convenient method for decomposing the energetics of donor–acceptor interactions from electronic structure calculations.^{33–35} The NBO analysis reveals that the strength of the internal $n(\text{N}) \rightarrow \sigma_{\text{CN}}^*$ interaction increases by approximately 3.1 kcal mol⁻¹ in the gas phase for **16** compared to **15** and is both basis set and correlation level independent. This striking energetic stabilization results from the increased acceptor strength of the σ_{CN}^* required to offset the electron density transferred to the approaching σ_{NH}^* .

The length of the hydrogen bond between the amina lone-pair and ammonium ion is found to be 1.7 and 1.748 Å at the RHF and MP2 levels of theory. If the intermolecular $n(\text{N}) \rightarrow \sigma_{\text{NH}}^*$ delocalisation were absent, the internal CN bond lengths should converge towards values more similar to those of **15** than those of complex **16**. Deletion of the intermolecular $n(\text{N}) \rightarrow \sigma_{\text{NH}}^*$ delocalisation within the NBO basis and re-optimization of **16** results in a dramatic lengthening of the hydrogen bond to nearly 2.9 Å. Since the $n(\text{N}) \rightarrow \sigma_{\text{NH}}^*$ interaction no longer moves electron density away from the nitrogen, the $n(\text{N}) \rightarrow \sigma_{\text{CN}}^*$ compensation effect is no longer required and the resulting geometry of **15** in the complex converges back to that observed for isolated **15**. This change in internal geometry

upon loss of the key $n(\text{N}) \rightarrow \sigma_{\text{NH}}^*$ interaction provides further evidence that the anomeric effect is strengthened upon coordination at nitrogen.

Conclusions

We have provided two examples of a hydrogen-bond induced structural anomeric effect in aminals, with the size of the bond length changes being affected by the strength of the hydrogen bond. Further protonation of **2** yields a dication **12** which undergoes ring opening/ring closure to an isomeric ion **13** via a monocyclic iminium ion, which can be trapped as a trication **14** in triflic acid.

Acknowledgements

We thank SERC for support through grant GR/D51834 and for a maintenance grant to R. W. M. We also thank Van B. Johnson for the original small-scale synthesis and characterisation of **6**.

References

- (a) R. U. Lemieux and N. J. Chü, Abstracts of Papers, *Am. Chem. Soc.*, 1958, **133**, 31N; (b) E. L. Eliel, *Angew. Chem., Int. Ed. Engl.*, 1972, **11**, 739 and references therein; (c) *Anomeric Effect: Origin and Consequences*, W. A. Szarek and D. Horton, Eds., ACS Symposium Series, Vol. 87, ACS publications, Washington, D. C., 1979.
- A. J. Kirby, *The Anomeric Effect and Related Stereoelectronic Effects at Oxygen*, Springer-Verlag, 1983.
- P. Deslongchamps, *Stereoelectronic Effects in Organic Chemistry*, Pergamon Press, Oxford, 1983.
- I. Tvaroska and T. Bleha, *Adv. Carbohydr. Chem. Biochem.*, R. S. Tipson and D. Horton, Eds., 1989, **47**, 45.
- The Anomeric Effect and Associated Stereoelectronic Effects*, Ed. G. R. J. Thatcher, ACS Symposium Series No. **539**, 1993.
- P. P. Graczyk and M. Mikołajczyk, *Top. Stereochem.*, 1994, **21**, 159.
- E. Juaristi and G. Cuevas, *The Anomeric Effect*, CRC Press, 1995.
- P. A. Petillo and L. E. Lerner, in reference 2, Ch. 9, p. 156.
- A. J. Kirby, *Acc. Chem. Res.*, 1984, **17**, 305.
- A. J. Kirby, *Adv. Phys. Org. Chem.*, 1994, **29**, 87.
- R. U. Lemieux and A. R. Morgan, *Can. J. Chem.*, 1965, **43**, 2205; R. U. Lemieux, *Pure Appl. Chem.*, 1971, **25**, 527; L. Hosie, P. J. Marshall and M. L. Sinnott, *J. Chem. Soc., Perkin Trans. 2*, 1984, 1121; W. G. Dauben and P. Kohler, *Carbohydr. Res.*, 1990, **203**, 47.
- C. L. Perrin and K. B. Armstrong, *J. Am. Chem. Soc.*, 1993, **115**, 6825; M. A. Fabian, C. L. Perrin and M. L. Sinnott, *ibid.*, 1994, **116**, 8398.
- P. G. Jones, A. J. Kirby, I. V. Komarov and P. D. Wothers, *Chem. Commun.*, 1998, 1695.
- E. J. Gabe, Y. Le Page, L. Prasad and G. R. Weisman, *Acta Crystallogr., Sect. B*, 1982, **38**, 2752.
- R. W. Alder, E. Heilbronner, E. Honegger, A. B. McEwen, R. E. Moss, E. Olefirowicz, P. A. Petillo, R. B. Sessions, G. R. Weisman, J. M. White and Z.-Z. Yang, *J. Am. Chem. Soc.*, 1993, **115**, 6580.
- This compound was also republished in 1996 without reference to the original work: T. Bailly, Y. Leroux, D. El Manouni, A. Neuman, T. Prangé and R. Burgada, *C. R. Acad. Sci. Paris, Ser. II*, 1996, **322**, 151; a correction has appeared, *ibid.*, 1996, **323**, 365.
- R. W. Alder, R. W. Mowlam, D. J. Vachon and G. R. Weisman, *J. Chem. Soc., Chem. Commun.*, 1992, 507.
- J. M. Erhardt and J. M. Wuest, *J. Am. Chem. Soc.*, 1980, **102**, 6363; T. J. Atkins, *J. Am. Chem. Soc.*, 1980, **102**, 6364; G. R. Weisman, V. B. Johnson and R. E. Fiala, *Tetrahedron Lett.*, 1980, **21**, 3635.
- G. M. Sheldrick, SHELXTL 5.1, Göttingen, 1985.
- International Tables for X-ray Crystallography, Vol. IV, (1974), Birmingham: Kynoch Press.
- F. Mohamadi, N. G. J. Richards, W. C. Guida, R. Liskamp, M. Lipton, C. Caufield, G. Chang, T. Hendrickson and W. C. Still, *J. Comput. Chem.*, 1990, **11**, 440.
- N. L. Allinger, *J. Am. Chem. Soc.*, 1977, **99**, 8127.
- (a) S. J. Weiner, P. A. Kollman, D. A. Case, U. C. Singh, C. Chio, G. Alagona, S. Profeta and P. Weiner, *J. Am. Chem. Soc.*, 1984, **106**, 765; (b) S. J. Weiner, P. A. Kollman and D. A. Case, *J. Comput. Chem.*, 1986, **7**, 230.
- D. M. Ferguson and P. A. Kollman, *J. Comput. Chem.*, 1991, **12**, 620.
- (a) W. Hasel, T. F. Hendrickson and W. C. Still, *Tetrahedron Comput. Method.*, 1988, **1**, 103; (b) W. C. Still, A. Tempczyk, R. C. Hawley and T. Hendrickson, *J. Am. Chem. Soc.*, 1990, **112**, 6127.

- 26 G. Chang, W. C. Guida and W. C. Still, *J. Am. Chem. Soc.*, 1989, **111**, 4379.
- 27 (a) J. J. P. Stewart, *J. Comput. Chem.*, 1989, **10**, 209; *ibid.*, 1989, **10**, 221.
- 28 Spartan V5.0: Wavefunction, Inc., 18401 Von Karman, Suite 370, Irvine, CA 92612, USA.
- 29 GAUSSIAN92, Revision A: M. J. Frisch, G. W. Trucks, M. Head-Gordon, P. M. W. Gill, M. W. Wong, J. B. Foresman, B. G. Johnson, H. B. Schlegel, M. A. Robb, E. S. Replogle, R. Gomperts, J. L. Andres, K. Raghavachari, J. S. Binkley, C. Gonzalez, R. L. Martin, D. J. Fox, D. J. Defrees, J. Baker, J. J. P. Stewart and J. A. Pople, Gaussian, Inc., Pittsburgh, PA, 1992.
- 30 GAUSSIAN94, Revision D.3: M. J. Frisch, G. W. Trucks, H. B. Schlegel, P. M. W. Gill, B. G. Johnson, M. A. Robb, J. R. Cheeseman, T. Keith, G. A. Petersson, J. A. Montgomery, K. Raghavachari, M. A. Al-Laham, V. G. Zakrzewski, J. V. Ortiz, J. B. Foresman, J. Cioslowski, B. B. Stefanov, A. Nanayakkara, M. Challacombe, C. Y. Peng, P. Y. Ayala, W. Chen, M. W. Wong, J. L. Andres, E. S. Replogle, R. Gomperts, R. L. Martin, D. J. Fox, J. S. Binkley, D. J. Defrees, J. Baker, J. J. P. Stewart, M. Head-Gordon, C. Gonzalez and J. A. Pople, Gaussian, Inc., Pittsburgh, PA, 1995.
- 31 (a) S. J. Huzinaga, *Chem. Phys.*, 1965, **42**, 1293; (b) T. H. Dunning, Jr., *J. Chem. Phys.*, 1971, **55**, 716; (c) T. H. Dunning and P. J. Hay, *Modern Theoretical Chemistry*, Plenum, New York, 1976, pp. 1–28.
- 32 T. Clark, J. Chandrasekhar, G. W. Spitznagel and P. v. R. Schleyer, *J. Comput. Chem.*, 1983, **3**, 294.
- 33 A. E. Reed, L. A. Curtiss and F. Weinhold, *Chem. Rev.*, 1988, **88**, 899.
- 34 NBO 4.0. E. D. Glendening, J. K. Badenhoop, A. E. Reed, J. E. Carpenter and F. Weinhold, Theoretical Chemistry Institute, University of Wisconsin, Madison, WI, USA, 1996.
- 35 P. A. Petillo, PhD Thesis, University of Wisconsin, Madison, 1991.
- 36 J. Dale, *Acta Chem. Scand.*, 1973, **27**, 1115; J. Dale, *Topics in Stereochemistry*, eds. N. L. Allinger and E. L. Eliel, Wiley, New York, 1976, vol. 9, pp. 199–270. Dale's nomenclature utilizes [abc...] to represent ring conformation, where a, b and c are each integers denoting the number of bonds between two true corners. A sequence of two gauche (synclinal) torsion angles introduces a bend; the atom flanked by these torsion angles is referred to as a true corner.
- 37 (a) H. Quast, B. Muller, E.-M. Peters, K. Peters and H. G. von Schnering, *Chem. Ber.*, 1982, **115**, 2752; (b) E. J. Gabe, L. Prasad, G. R. Weisman and V. B. Johnson, *Acta Crystallogr., Sect. C*, 1983, **39**, 275; (c) H. Kupperts, A. Samhammer and R. Haller, *Acta Crystallogr., Sect. C*, 1987, **43**, 1974; (d) A. H.-J. Wang, E. N. Duesler, N. N. Thayer, R. Heckendorn, K. L. Rinehart, Jr. and I. C. Paul, *Acta Crystallogr., Sect. B*, 1978, **34**, 2319; (e) I. L. Karle and J. Karle, *Acta Crystallogr.*, 1964 **17**, 1964; (f) N. W. Alcock, P. Moore and K. F. Mok, *J. Chem. Soc., Perkin Trans. 2*, 1980, 1186; (g) J. W. Fischer, R. A. Hollins, C. Klowe-Ma, R. A. Nissan and R. D. Chapman, *J. Org. Chem.*, 1996, **61**, 9340; (h) J. P. Dutasta, G. Gellon, J. L. Pierre, M. T. Averbuch-Pouchot and A. Durif, *Acta Crystallogr., Sect. C*, 1990, **46**, 259; (i) J.-L. Wang, M. Sun, F.-M. Miao, S.-Y. Wu, F.-S. Gong and X.-H. Duan, *Acta Crystallogr., Sect. C*, 1991, **47**, 2203; (j) J. K. Frank, E. N. Duesler, N. N. Thayer, R. Heckendorn, K. L. Rinehart, Jr., I. C. Paul and R. Misra, *Acta Crystallogr., Sect. B*, 1978, **34**, 2316; (k) H. R. Howard, K. D. Shenk, K. C. Coffman, D. K. Bryce, R. T. Crawford and S. A. McLean, *Bioorg. Med. Chem. Lett.*, 1995, **5**, 111.
- 38 P. G. Jones, *Chem. Soc. Rev.*, 1984, **13**, 157.
- 39 F. H. Allen, L. Brammer, O. Kennard, A. G. Orpen, R. Taylor and D. G. Watson, *J. Chem. Soc., Perkin Trans. 2*, 1987, S1–S19.
- 40 R. W. Alder, B. J. Dunne, K. Marsden, A. G. Orpen and J. M. White, to be submitted.
- 41 R. W. Alder, A. G. Orpen and J. M. White, *Acta Crystallogr., Sect. C*, 1988, **44**, 287.
- 42 J. M. White, R. W. Alder and A. G. Orpen, *Acta Crystallogr., Sect. C*, 1988, **44**, 872.
- 43 R. W. Alder, P. Eastment, N. M. Hext, R. E. Moss, A. G. Orpen and J. M. White, *J. Chem. Soc., Chem. Commun.*, 1988, 1528.
- 44 R. W. Alder, A. G. Orpen and R. B. Sessions, *J. Chem. Soc., Chem. Commun.*, 1983, 999. For a correction to the space group see W. B. Schaefer and R. E. Marsh, *J. Chem. Soc., Chem. Commun.*, 1984, 1555.
- 45 R. W. Alder, R. E. Moss and R. B. Sessions, *J. Chem. Soc., Chem. Commun.*, 1983, 1000.
- 46 A. R. Mahjoub, D. Leopold and K. Seppelt, *Z. Anorg. Allg. Chem.*, 1992, **618**, 83.
- 47 G. I. Birnbaum, K. K. Cheung, M. Wiewiorowski and M. D. Bratek-Wiewiorowska, *J. Chem. Soc. B*, 1967, 1368.
- 48 A. V. Goncharov, V. N. Panov, A. V. Maleyev, K. A. Potekhin, Ye. N. Kurkutova, Yu. T. Struchkov, V. A. Palyulin and N. S. Zefirov, *Dokl. Akad. Nauk SSSR*, 1991, **318**, 907.
- 49 E. Weber, U. Muller, D. Worsch, F. Vogtle, G. Will and A. Kirfel, *J. Chem. Soc., Chem. Commun.*, 1985, 1578.